

Theory of Quantum Imaging with Undetected Photons

Mayukh Lahiri,^{1,*} Radek Lapkiewicz,¹ Gabriela Barreto Lemos,¹ and Anton Zeilinger^{1,2}

¹*Vienna Center for Quantum Science and Technology (VCQ), Faculty of Physics,
Boltzmannngasse 5, University of Vienna, Vienna A-1090, Austria.*

²*Institute for Quantum Optics and Quantum Information,
Austrian Academy of Sciences, Boltzmannngasse 3, Vienna A-1090, Austria.*

Abstract: A novel quantum imaging technique has recently been demonstrated in an experiment, where the photon used for illuminating an object is not detected; the image is obtained by interfering two beams, none of which ever interacts with the object. Here we present a detailed theoretical analysis of the experiment. We show that the object information is present only in the interference term and not in the individual intensities of the interfering beams. We also theoretically establish that the magnification of the imaging system depends on two wavelengths: the average wavelength of the photon that illuminates the object and the average wavelength of the photon that is detected. Our analysis affirms that the imaging process is based on the principle that quantum interference occurs when interferometric path information is unavailable.

I. INTRODUCTION

According to Bohr, comprehending the nature of a quantum system requires “a combined use of the contrasting pictures” of a classical particle and a classical wave [1]. Bohr’s complementarity principle [2] implies that the complete particle behavior and the complete wave behavior of a quantum system or entity are mutually exclusive. In other words, if a quantum entity behaves completely like a particle (wave) under certain experimental conditions, it does not display its wave (particle) behavior under the same conditions. To avoid confusion, we do not refer to a quantum entity as either “particle” or “wave”; instead, we use the term “quanton” (see, for example, [3]).

The wave-particle duality can be illustrated by a lowest-order [4] interference experiment (e.g., Young’s double-slit experiment, Mach-Zehnder interferometer, etc.), in which a single quanton (e.g., photon, electron, etc.) is sent into a two-way interferometer (see, for example, [5]). If the quanton behaves completely like a particle, no interference can be observed at the output of the interferometer. It turns out that in this case it is possible to determine with complete certainty via which path the quanton has traversed. On the other hand, when there is absolutely no information on the path traveled by the quanton, perfect interference occurs—a behavior that characterizes waves. The relationship between interference and path information (wave-particle duality) has drawn the attention of several researchers (see, for example, [6–10]).

The imaging process [11] of our interest is related to the wave-particle duality of photons. Let us consider two spatially separated identical light sources, 1 and 2, each of which has the ability of producing two photons at a time. These two photons are, in general, not identical

with each other and we label them by a and b . Suppose now that we select the a -photons from the both sources and send them into a two-arm interferometer under the following conditions: 1) photons from a particular source can travel through only one of the arms; 2) the sources emit at the same rate but in such a way that there is never more than one photon present in the interferometer at a time. In this case, although the a -photons are identical with each other, one can partially or fully extract the interferometric path information by interacting with a b -photon that is not sent into the interferometer. In such a situation, it is, therefore, possible to control the interference of a photon sent into the interferometer by using a photon that is not sent into the interferometer. This phenomenon has been experimentally demonstrated and discussed in Refs. [12, 13] and is often referred to as “induced coherence without induced emission”.

The essence of our imaging technique [11] lies in the fact that the effect of interaction with b -photons is observed in the first-order interference fringe pattern produced by the a -photons. As for sources, we use two identical nonlinear crystals which generate photons by spontaneous parametric down-conversion. In Section II, we briefly recapitulate some basic results relating to the theory of spontaneous parametric down-conversion. In Section III, we then present a detailed analysis of the imaging method. Finally, we summarize our results in Section IV.

II. ELEMENTS OF THE THEORY OF SPONTANEOUS PARAMETRIC DOWN-CONVERSION

We mostly follow the theory of the process of spontaneous parametric down-conversion developed by Hong and Mandel [14]. In this process a nonlinear crystal converts a photon (pump) into two photons (signal and idler) each of which has energy lower than that of the pump-photon. The combined energy of the signal and the idler photons is equal to the energy of the pump-photon.

*Electronic address: mayukh.lahiri@univie.ac.at

When the pump beam is highly coherent and the down-conversion does not bring any observable change in the pump intensity, one can represent the pump by a classical electric field $\mathbf{E}_P(\mathbf{r}, t)$. In this case, the interaction Hamiltonian associated with the process of parametric down-conversion can be expressed in the interaction picture as (cf. [13, 14])

$$\begin{aligned} \hat{H}_{in}(t) \\ = \int_D d^3r \tilde{\chi}_{lmq} E_{Pl}(\mathbf{r}, t) \hat{E}_{Sm}^{(-)}(\mathbf{r}, t) \hat{E}_{Iq}^{(-)}(\mathbf{r}, t) + \text{H.c.}, \end{aligned} \quad (1)$$

where $\tilde{\chi}$ represents the nonlinear electric susceptibility tensor of the crystal, $\hat{\mathbf{E}}_S^{(-)}(\mathbf{r}, t)$ and $\hat{\mathbf{E}}_I^{(-)}(\mathbf{r}, t)$ are the negative frequency parts of the quantized electric fields associated with the signal and idler, respectively, D is the volume of the crystal, H.c. implies Hermitian conjugation, and there is summation over the repeated indices l, m, q which label three mutually orthogonal directions in space.

The pump, the signal and the idler fields may oscillate at different optical frequencies. In general, the susceptibility of the crystal depends on these frequencies. The Hamiltonian in Eq. (1) is therefore often expressed by decomposing the optical fields into several modes (see, for example, [14]). The positive frequency part of a quantized electric field inside the crystal can be represented by the expression [15]

$$\hat{\mathbf{E}}^{(+)}(\mathbf{r}, t) = \sum_{\mathbf{k}, \sigma} \alpha(\mathbf{k}, \sigma) \exp[i(\mathbf{k} \cdot \mathbf{r} - \omega t)] \mathbf{e}_{\mathbf{k}, \sigma} \hat{a}(\mathbf{k}, \sigma), \quad (2)$$

where $\sigma = 1, 2$, labels two directions of polarization, ω is the frequency, \mathbf{k} is the wave vector, $\mathbf{e}_{\mathbf{k}, \sigma}$ represents two generally complex, mutually orthogonal unit vectors such that $\mathbf{e}_{\mathbf{k}, \sigma} \cdot \mathbf{k} = 0$, $\alpha(\mathbf{k}, \sigma) = i\sqrt{\hbar\omega/(2\epsilon_0 n^2(\mathbf{k}, \sigma)L^3)}$, ϵ_0 is the electric permittivity of free space, $n(\mathbf{k}, \sigma)$ is the refractive index of the anisotropic, nonlinear crystal, L^3 is the quantization volume, and $\hat{a}(\mathbf{k}, \sigma)$ is the photon annihilation operator for the mode labeled by (\mathbf{k}, σ) . Let us also decompose the pump field inside the crystal into plane wave modes and express it in the form

$$\mathbf{E}_P(\mathbf{r}, t) = \sum_{\mathbf{k}_P, \sigma_P} V_P(\mathbf{k}_P, \sigma_P) \exp[i(\mathbf{k}_P \cdot \mathbf{r} - \omega_P t)] \mathbf{e}_{\mathbf{k}_P, \sigma_P}. \quad (3)$$

The Hamiltonian, given by Eq. (1), now takes the form

(cf. [16])

$$\begin{aligned} \hat{H}_{in}(t) \\ = \int_D d^3r \sum_{\mathbf{k}_P, \sigma_P} \sum_{\mathbf{k}_S, \sigma_S} \sum_{\mathbf{k}_I, \sigma_I} \left\{ \chi_{lmq}(\omega_P, \omega_S, \omega_I) V_P(\mathbf{k}_P, \sigma_P) \right. \\ \left. (\mathbf{e}_{\mathbf{k}_P, \sigma_P})_l (\mathbf{e}_{\mathbf{k}_S, \sigma_S}^*)_m (\mathbf{e}_{\mathbf{k}_I, \sigma_I}^*)_q \alpha^*(\mathbf{k}_S, \sigma_S) \alpha^*(\mathbf{k}_I, \sigma_I) \right. \\ \left. \exp[i(\omega_S + \omega_I - \omega_P)t] \exp[i(\mathbf{k}_P - \mathbf{k}_S - \mathbf{k}_I) \cdot \mathbf{r}] \right. \\ \left. \hat{a}_S^\dagger(\mathbf{k}_S, \sigma_S) \hat{a}_I^\dagger(\mathbf{k}_I, \sigma_I) \right\} + \text{H.c.}, \end{aligned} \quad (4)$$

where the subscripts P, S and I refer to pump, signal and idler, respectively. The quantum state of light generated by down-conversion at the crystal is given by the well known formula

$$|\psi(t')\rangle = \exp\left[\frac{1}{i\hbar} \int_0^{t'} dt \hat{H}_{in}(t)\right] |\text{vac}\rangle, \quad (5)$$

where $|\text{vac}\rangle$ is the vacuum state and t' is the interaction time. By expanding the exponential, Eq. (5) can be expressed in the form

$$|\psi(t')\rangle = |\text{vac}\rangle + \left[\frac{1}{i\hbar} \int_0^{t'} dt \hat{H}_{in}(t)\right] |\text{vac}\rangle + \dots \quad (6)$$

III. IMAGING

Let us consider a situation in which two identical nonlinear crystals NL1 and NL2 are pumped by optical beams P_1 and P_2 , respectively, generated by the same laser source (Fig. 1). The idler beam, I_1 , generated by NL1

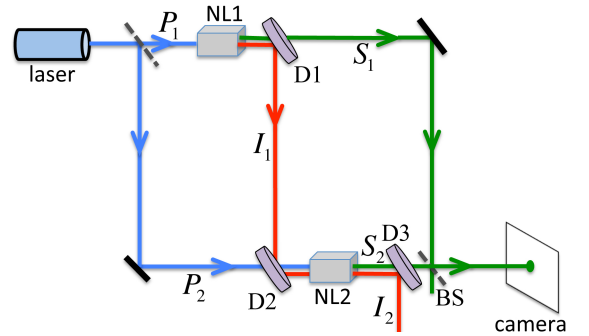


FIG. 1: Illustrating the principle of the experiment. A laser beam (blue) is split into two beams P_1 and P_2 which pump the nonlinear crystals NL1 and NL2. The crystals produce signal (green) and idler (red) beams. The idler beam I_1 is aligned with the idler beam I_2 . The signal beams S_1 and S_2 are superposed by the beam splitter BS and one of the outputs of BS is detected by a camera. D1, D2, D3 are dichroic mirrors.

is transmitted through NL2 and is aligned with the idler beam, I_2 , generated by the latter. The signal beams S_1

and S_2 from the crystals NL1 and NL2, respectively, are superposed by a beam-splitter, BS. One of the outputs of the beam-splitter is detected by an EMCCD camera.

Suppose that the pump fields at the two crystals are given by the complex electric field vectors $\mathbf{E}_{P_1}(\mathbf{r}_1, t_2)$ and $\mathbf{E}_{P_2}(\mathbf{r}_2, t_2)$, expanded in the form given by Eq. (3). From Eqs. (2), (3), (4) and (6) it follows that the quantum state of light generated by each individual crystal is given by the formula (cf. [17])

$$\begin{aligned}
 |\psi_j(t')\rangle &= |\text{vac}\rangle + \frac{t'D}{i\hbar} \sum_{\mathbf{k}_{P_j}, \sigma_{P_j}} \sum_{\mathbf{k}_{S_j}, \sigma_{S_j}} \sum_{\mathbf{k}_{I_j}, \sigma_{I_j}} \left[\chi_{lmq}(\omega_{P_j}; \omega_{S_j}, \omega_{I_j}) \right. \\
 &\quad V_{P_j}(\mathbf{k}_{P_j}, \sigma_{P_j}) \alpha^*(\mathbf{k}_{S_j}, \sigma_{S_j}) \alpha^*(\mathbf{k}_{I_j}, \sigma_{I_j}) \left(\mathbf{e}_{\mathbf{k}_{P_j}, \sigma_{P_j}} \right)_l \\
 &\quad \left(\mathbf{e}_{\mathbf{k}_{S_j}, \sigma_{S_j}} \right)_m \left(\mathbf{e}_{\mathbf{k}_{I_j}, \sigma_{I_j}} \right)_q \exp \left[i(\omega_{S_j} + \omega_{I_j} - \omega_{P_j})t'/2 \right] \\
 &\quad \text{sinc}[(\omega_{S_j} + \omega_{I_j} - \omega_{P_j})t'/2] \\
 &\quad \exp \left[i(\mathbf{k}_{P_j} - \mathbf{k}_{S_j} - \mathbf{k}_{I_j}) \cdot \mathbf{r}_{0_j} \right] \\
 &\quad \left\{ \prod_{n=1}^3 \text{sinc}[(\mathbf{k}_{P_j} - \mathbf{k}_{S_j} - \mathbf{k}_{I_j})_n l_n/2] \right\} \\
 &\quad \left. |\mathbf{k}_{S_j}, \sigma_{S_j}\rangle_{S_j} |\mathbf{k}_{I_j}, \sigma_{I_j}\rangle_{I_j} \right] + \dots, \quad (7)
 \end{aligned}$$

where $j = 1, 2$ labels the two crystals, $|\mathbf{k}_{S_j}, \sigma_{S_j}\rangle_{S_j} = \hat{a}_{S_j}^\dagger(\mathbf{k}_{S_j}, \sigma_{S_j}) |\text{vac}\rangle_{S_j}$, $|\mathbf{k}_{I_j}, \sigma_{I_j}\rangle_{I_j} = \hat{a}_{I_j}^\dagger(\mathbf{k}_{I_j}, \sigma_{I_j}) |\text{vac}\rangle_{I_j}$, the volume integration has been carried out assuming the crystal to be a rectangular parallelepiped [18] of sides l_1, l_2, l_3 with its center located at the point \mathbf{r}_{0_j} , and $\text{sinc}[x] = \sin x/x$; the sinc terms lead to the two well known phase matching conditions associated with the process of spontaneous parametric down-conversion.

A. Alignment of Idler Beams

If the beam I_1 is perfectly aligned with the beam I_2 , for each mode present in the quantized field $\hat{\mathbf{E}}_{I_1}^{(+)}$ of I_1 there exists an equally populated mode in the quantized field $\hat{\mathbf{E}}_{I_2}^{(+)}$ of I_2 . The perfect alignment of the idler beams can, therefore, be analytically expressed by the following formula:

$$\hat{a}_{I_2}(\mathbf{k}_I, \sigma_I) = \hat{a}_{I_1}(\tilde{\mathbf{k}}_I, \tilde{\sigma}_I) \exp[i\phi_I(\tilde{\mathbf{k}}_I, \tilde{\sigma}_I)], \quad (8)$$

where the mode $(\tilde{\mathbf{k}}_I, \tilde{\sigma}_I)$ is generated at NL1 and is aligned with the mode (\mathbf{k}_I, σ_I) that is generated at NL2; $\phi_I(\tilde{\mathbf{k}}_I, \tilde{\sigma}_I)$ is a phase factor which can be interpreted as the phase gained by the mode $(\tilde{\mathbf{k}}_I, \tilde{\sigma}_I)$ due to propagation from NL1 to NL2.

The Hamiltonian given by Eq. (4) and, consequently, the state in Eq. (7) are expressed in quite general forms. We now simplify them using certain assumptions which

are appropriate to our experiment. Let us assume that the signal and the idler can be treated as beams with uniform linear polarization both inside and outside of the crystals. In such a situation, we can drop the summation over the polarization indices $\sigma_{P_j}, \sigma_{S_j}, \sigma_{I_j}$ and can also write

$$\alpha(\mathbf{k}_{S_j}, \sigma_{S_j}) \approx \alpha_S(\omega_{S_j}), \quad \alpha(\mathbf{k}_{I_j}, \sigma_{I_j}) \approx \alpha_I(\omega_{I_j}), \quad (9)$$

One can now replace the annihilation operator $\hat{a}(\mathbf{k}, \sigma)$ with $\hat{a}(\mathbf{k})$, the number state $|\mathbf{k}, \sigma\rangle$ with $|\mathbf{k}\rangle$ and the susceptibility tensor χ_{lmq} with a scalar quantity χ . Furthermore, the alignment condition given by Eq. (8) reduces to the form

$$\hat{a}_{I_2}(\mathbf{k}_I) = \hat{a}_{I_1}(\tilde{\mathbf{k}}_I) \exp[i\phi_I(\tilde{\mathbf{k}}_I)]. \quad (10)$$

It is to be noted that the relationship between $\tilde{\mathbf{k}}_I$ and \mathbf{k}_I depends on the optical system used for aligning the idler beams.

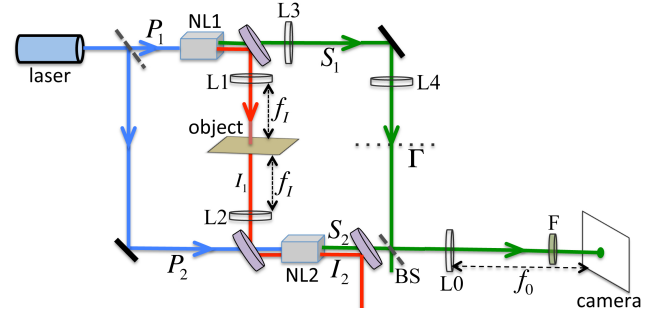


FIG. 2: Schematics of the imaging experiment. Positive lenses L1 and L2 (both of focal length f_I), placed in the path of I_1 , form a 4-f system that images NL1 on NL2. An identical 4-f system, consisting of positive lenses L3 and L4, is placed in the path of S_1 . A thin object is placed on a plane which is the back focal plane of L1 and the front focal plane of L2. One of the outputs of BS is focused by a positive lens L0 of focal length f_0 into a camera. NL2 and the back focal plane, Γ , of L4 are located at the front focal plane of L0. The lenses are assumed to be thin and ideal. The superposed signal beam is passed through a narrow-band filter, F, before entering the camera.

In the experiment the two idler beams are aligned by the use of a 4-f lens system that images a central plane of NL1 onto a central plane of NL2 (Fig. 2). We assume the idler beam axis to be along the optical axis of the lens system. A thin object which is intended to be imaged is placed at the back focal plane of the first positive lens, L1, of the 4-f system; this plane is also the front focal plane of the second positive lens, L2, of the same 4-f system. Clearly, the object is illuminated only by the idler beam that is generated by the first crystal.

If a plane wave characterized by the wave vector $\tilde{\mathbf{k}}_I$ is incident on L1, it gets converted into a spherical wave that converges to a point $\rho_{\tilde{\mathbf{k}}_I}$, say, on the back focal plane of L1 [Fig. 3(a)]. It then reemerges from this point as a

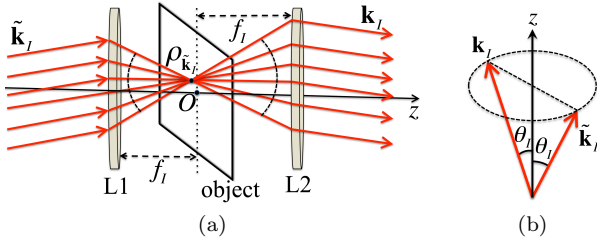


FIG. 3: Illustrating notations: (a) $\rho_{\tilde{\mathbf{k}}_I}$ is a two-dimensional position vector lying on the object plane. The origin is chosen at the point O where the optical axis z meets the object plane. We neglect the limits due to diffraction. (b) The wave vectors $\tilde{\mathbf{k}}_I$ and \mathbf{k}_I are mirror images of each other with respect to the optical axis z . θ_I is the absolute value of the angle they make with the optical axis.

diverging spherical wave. The amplitude of the diverging spherical wave can be determined from the amplitude of the incident wave and the complex transmission coefficient $\mathcal{T}(\rho_{\tilde{\mathbf{k}}_I})$ of the object at point $\rho_{\tilde{\mathbf{k}}_I}$. The diverging spherical wave gets reconverted into a plane wave by the positive lens L2. This plane wave is characterized by a wave vector \mathbf{k}_I which is different from $\tilde{\mathbf{k}}_I$, unless $\tilde{\mathbf{k}}_I$ is along the optical axis z of the lens system. If one neglects the limits due to diffraction, one can say that a plane wave emerging from L2 contains information about one specific point of the object.

Although the discussion of the previous paragraph is applicable to a classical field, it provides a guideline for treating the problem quantum mechanically. Since a quantized field is represented by decomposing it into several plane wave modes, one can say that one point on the object can transmit and reflect only one specific mode of the quantized idler field. Hence a single point on the object acts as a beam splitter only on one particular idler mode. Using the quantum mechanical treatment of a beam splitter ([19], sec. 12.12), one can now write the alignment condition [Eq. (10)] in the following form:

$$\hat{a}_{I_2}(\mathbf{k}_I) = \left[\mathcal{T}(\rho_{\tilde{\mathbf{k}}_I}) \hat{a}_{I_1}(\tilde{\mathbf{k}}_I) + \mathcal{R}'(\rho_{\tilde{\mathbf{k}}_I}) \hat{a}_0(\tilde{\mathbf{k}}_I) \right] \times \exp[i\phi_I(\tilde{\mathbf{k}}_I)], \quad (11)$$

where $\mathcal{T}(\rho_{\tilde{\mathbf{k}}_I})$ is the transmission coefficient of the object at the point $\rho_{\tilde{\mathbf{k}}_I}$, $\mathcal{R}'(\rho_{\tilde{\mathbf{k}}_I})$ is the reflection coefficient at the same point when illuminated from the opposite direction, \hat{a}_0 represents the vacuum field at the unused port of the beam splitter (a point on the object), $\phi_I(\tilde{\mathbf{k}}_I)$ is the phase term mentioned earlier and $|\mathcal{T}|^2 + |\mathcal{R}'|^2 = 1$. It is evident that in absence of the object, i.e., when $\mathcal{T} = 1$ and $\mathcal{R}' = 0$, Eq. (11) reduces to Eq. (10).

If one neglects the limits due to diffraction, there is an one-to-one correspondence between \mathbf{k}_I and $\tilde{\mathbf{k}}_I$, i.e., for every choice of \mathbf{k}_I there is one and only one $\tilde{\mathbf{k}}_I$. When the focal lengths of L1 and L2 are equal, \mathbf{k}_I and $\tilde{\mathbf{k}}_I$ are mirror images of each other with respect to the optical axis z [see Fig. 3(b)].

B. Detection System

Let us now consider the detection system used in the experimental setup. The signal beams generated by the two crystals are superposed by a 50 : 50 beam splitter (BS) and one of the outputs of the beam splitter is focused on an EMCCD camera by a positive lens L0 (Fig. 2). A filter, F, is placed in front of the camera so that the light entering the camera has a narrow frequency band of mean frequency $\bar{\omega}_S$.

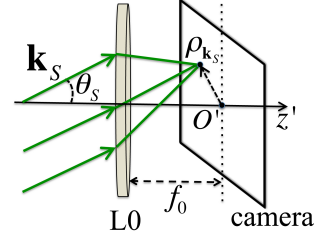


FIG. 4: Illustrating notations relating to the detection system: $\rho_{\mathbf{k}_S}$ is a two-dimensional position vector lying on the image plane (camera screen). The origin is chosen at the point O' where the optical axis (also the beam axis) z' meets the image plane. The wave vector \mathbf{k}_S makes an angle θ_S with the optical axis.

In absence of limits due to diffraction, L0 would focus a plane wave with wave vector \mathbf{k}_S at a point $\rho_{\mathbf{k}_S}$, say, on the camera screen (Fig. 4). Hence the positive frequency part of the quantized field at the camera can be expressed as [20]

$$\begin{aligned} \hat{E}_S^{(+)}(\rho_{\mathbf{k}_S}, t) &\propto \exp \left[-i\bar{\omega}_S \left(t - \frac{L_1(\mathbf{k}_S)}{c} \right) \right] \hat{a}_{S_1}(\mathbf{k}_S) \\ &+ i \exp \left[i\mathbf{k}_S \cdot \mathbf{r}_0 - i\bar{\omega}_S \left(t - \frac{L_2(\mathbf{k}_S)}{c} \right) \right] \hat{a}_{S_2}(\mathbf{k}_S), \end{aligned} \quad (12)$$

where $L_j(\mathbf{k}_S)$ is the optical path traveled by the mode labeled by \mathbf{k}_S from the nonlinear crystal j to the camera (propagation inside the crystals has been neglected), $|\mathbf{k}_S| = \bar{\omega}_S/c$ and we have chosen $\mathbf{r}_{0_1} = 0$, $\mathbf{r}_{0_2} - \mathbf{r}_{0_1} = \mathbf{r}_0$.

C. Formation of an Image

For the sake of simplicity, we assume that the pump beams are well collimated, uniformly polarized and narrow-band with mean frequency $\bar{\omega}_P$. In this case, the pump field at the crystal j can be represented by $V_{P_j} \exp[i(\mathbf{k}_P \cdot \mathbf{r} - \bar{\omega}_P t)]$. We choose the direction of \mathbf{k}_P to be along the direction of the optical axis. Using Eqs. (7), (9) and (11) one can show (see Appendix 1) that the quantum state of the field in this system can be approx-

imated by

$$\begin{aligned}
|\Psi\rangle \approx & |\text{vac}\rangle + \frac{t'D}{i\hbar} \sum_{\mathbf{k}_{S_1}} \sum_{\mathbf{k}_{I_1}} \left[g(\omega_{S_1}, \omega_{I_1}) V_{P_1} \right. \\
& \left. \left\{ \prod_{n=1}^3 \text{sinc}[(\mathbf{k}_P - \mathbf{k}_{S_1} - \mathbf{k}_{I_1})_n l_n / 2] \right\} \right. \\
& \left. \text{sinc}[(\omega_{S_1} + \omega_{I_1} - \bar{\omega}_P)t'/2] |\mathbf{k}_{S_1}\rangle_{S_1} |\mathbf{k}_{I_1}\rangle_{I_1} |0\rangle_{S_2} |0\rangle_0 \right] \\
& + \frac{t'D}{i\hbar} \sum_{\mathbf{k}_{S_2}} \sum_{\mathbf{k}_{I_2}} \left[g(\omega_{S_2}, \omega_{I_2}) V_{P_2} \exp[i(\mathbf{k}_P - \mathbf{k}_{S_2} - \mathbf{k}_{I_2}) \cdot \mathbf{r}_0] \right. \\
& \left. \exp[-i\phi_I(\tilde{\mathbf{k}}_{I_2})] \text{sinc}[(\omega_{S_2} + \omega_{I_2} - \bar{\omega}_P)t'/2] \right. \\
& \left. \left\{ \prod_{n=1}^3 \text{sinc}[(\mathbf{k}_P - \mathbf{k}_{S_2} - \mathbf{k}_{I_2})_n l_n / 2] \right\} \right. \\
& \left. \left(\mathcal{T}^*(\boldsymbol{\rho}_{\tilde{\mathbf{k}}_{I_2}}) |0\rangle_{S_1} |\tilde{\mathbf{k}}_{I_2}\rangle_{I_1} |\mathbf{k}_{S_2}\rangle_{S_2} |0\rangle_0 \right. \right. \\
& \left. \left. + \mathcal{R}'^*(\boldsymbol{\rho}_{\tilde{\mathbf{k}}_{I_2}}) |0\rangle_{S_1} |0\rangle_{I_1} |\mathbf{k}_{S_2}\rangle_{S_2} |\tilde{\mathbf{k}}_{I_2}\rangle_0 \right) \right], \quad (13)
\end{aligned}$$

where $g(\omega_{S_j}, \omega_{I_j}) = \chi(\omega_{S_j}, \omega_{I_j}) \alpha_S^*(\omega_{S_j}) \alpha_I^*(\omega_{I_j}) \exp[i(\omega_{S_j} + \omega_{I_j} - \bar{\omega}_P)t'/2]$, $\tilde{\mathbf{k}}_{I_2}$ is the mirror image of \mathbf{k}_{I_2} with respect to the optical axis (beam axis) of the 4-f system and we have suppressed the normalization coefficients. In the experiment, we choose crystals whose sides are approximately 10^{-3}m of length; since the wave vectors are characterized by corresponding optical wavelengths, the terms $\text{sinc}[(\mathbf{k}_{P_j} - \mathbf{k}_{S_j} - \mathbf{k}_{I_j})_n l_n / 2]$ in Eq. (7) contribute only when $\mathbf{k}_{P_j} - \mathbf{k}_{S_j} - \mathbf{k}_{I_j} \approx 0$. This implies that the spatial phase matching condition $\mathbf{k}_{P_j} \approx \mathbf{k}_{S_j} + \mathbf{k}_{I_j}$ holds to a very good accuracy. Furthermore, the term $\text{sinc}[(\omega_{S_j} + \omega_{I_j} - \bar{\omega}_P)t'/2]$ leads to the temporal phase matching condition $\bar{\omega}_P \approx \omega_{S_j} + \omega_{I_j}$.

The photon counting rate [21] at a point $\boldsymbol{\rho}_{\mathbf{k}_S}$ in the camera is given by

$$\mathcal{R}(\boldsymbol{\rho}_{\mathbf{k}_S}) \propto \langle \Psi | \hat{E}_S^{(-)}(\boldsymbol{\rho}_{\mathbf{k}_S}, t) \hat{E}_S^{(+)}(\boldsymbol{\rho}_{\mathbf{k}_S}, t) | \Psi \rangle, \quad (14)$$

where $|\Psi\rangle$ is given by Eq. (13) and the quantized field is given by Eq. (12). It follows from a long but straightforward calculation that apart from a proportionality constant $\mathcal{R}(\boldsymbol{\rho}_{\mathbf{k}_S})$ is given by

$$\begin{aligned}
\mathcal{R}(\boldsymbol{\rho}_{\mathbf{k}_S}) \approx & |V_{P_1}|^2 + |V_{P_2}|^2 \\
& + 2|V_{P_1}||V_{P_2}||\mathcal{T}(\boldsymbol{\rho}_{\tilde{\mathbf{k}}_I})| \\
& \cos \left[\phi_{S_2}(\mathbf{k}_S) - \phi_{S_1}(\mathbf{k}_S) - \phi_I(\tilde{\mathbf{k}}_I) \right. \\
& \left. - \arg[\mathcal{T}(\boldsymbol{\rho}_{\tilde{\mathbf{k}}_I})] + \phi_P + \mathbf{k}_S \cdot \mathbf{r}_0 + C_0 \right], \quad (15)
\end{aligned}$$

where $\tilde{\mathbf{k}}_I$ denotes a wave vector that is the mirror image of the wave vector $\mathbf{k}_I = \mathbf{k}_P - \mathbf{k}_S$ with respect to the optical axis [Fig. 3(b)], $|\mathbf{k}_P| = \bar{\omega}_P/c$, $|\mathbf{k}_S| = \bar{\omega}_S/c$, $|\mathbf{k}_I| = \bar{\omega}_I/c$, $\boldsymbol{\rho}_{\tilde{\mathbf{k}}_I}$ is the point on the object that is illuminated by the idler mode $\tilde{\mathbf{k}}_I$, $\phi_{S_j}(\mathbf{k}_S) = \bar{\omega}_S L_j(\mathbf{k}_S)/c$,

$\phi_P = \arg[V_{P_2}] - \arg[V_{P_1}]$, and C_0 includes all other phase terms. Equation (15) is the key equation of the theory of imaging.

Let us first consider the situation in which no object is placed in the idler's path, i.e., when $|\mathcal{T}| = 1$ and $\arg[\mathcal{T}] = 0$. We have already mentioned in Section IIIB that a point on the image plane (camera) has contribution only from one signal mode \mathbf{k}_S . Since the diameter of the signal beam cross-section in the camera is much smaller in dimension than the optical paths $L_j(\mathbf{k}_S)$ and the distance $|\mathbf{r}_0|$ between the two crystals, the terms $\mathbf{k}_S \cdot \mathbf{r}_0$ and $\phi_{S_j}(\mathbf{k}_S)$ can be treated as a slowly varying function of \mathbf{k}_S . Similarly, since the diameter of the first idler beam inside NL2 is much smaller than the distance between the two crystals, one can also neglect the $\tilde{\mathbf{k}}_I$ dependence of $\phi_I(\tilde{\mathbf{k}}_I)$. These allow us to write $\phi_{S_2}(\mathbf{k}_S) - \phi_{S_1}(\mathbf{k}_S) \approx \Delta_{S0}$, $\phi_I(\tilde{\mathbf{k}}_I) \approx \phi_{I0}$ and $\mathbf{k}_S \cdot \mathbf{r}_0 + C_0 \approx C'_0$, where Δ_{S0} , ϕ_{I0} and C'_0 are constants. Equation (15) now reduces to

$$\begin{aligned}
\mathcal{R}(\boldsymbol{\rho}_{\mathbf{k}_S}) \approx & |V_{P_1}|^2 + |V_{P_2}|^2 \\
& + 2|V_{P_1}||V_{P_2}| \cos \left[\Delta_{S0} - \phi_{I0} + \phi_P + C'_0 \right]. \quad (16)
\end{aligned}$$

Since the right-hand side of Eq. (16) does not have any \mathbf{k}_S dependence, it is clear that an almost uniformly illuminated beam cross-section would be observed in the camera. The phase term ϕ_P can be controlled in the experiment and by doing so one can modulate the intensity of the beam spot. It is evident from Eq. (16) that by changing the value of ϕ_P , one can achieve conditions both of constructive and of destructive interference, which are given by the following equations, respectively:

$$\Delta_{S0} - \phi_{I0} + \phi_{PC} + C'_0 = 2N\pi, \quad (17a)$$

$$\Delta_{S0} - \phi_{I0} + \phi_{PD} + C'_0 = (2N + 1)\pi, \quad (17b)$$

where ϕ_{PC} and ϕ_{PD} are values of ϕ_P for constructive and destructive interferences [22], respectively, and N is an integer. Thus we have established the relations

$$\phi_{S_2}(\mathbf{k}_S) - \phi_{S_1}(\mathbf{k}_S) - \phi_I(\tilde{\mathbf{k}}_I) + \phi_{PC} + C'_0 \approx 2N\pi, \quad (18a)$$

$$\phi_{S_2}(\mathbf{k}_S) - \phi_{S_1}(\mathbf{k}_S) - \phi_I(\tilde{\mathbf{k}}_I) + \phi_{PD} + C'_0 \approx (2N + 1)\pi. \quad (18b)$$

When the object is inserted in the idler's path, it follows from Eqs. (15) and (18) that the photon counting rates at a point in the camera under the conditions of constructive and destructive interference are, respectively, given by the formulas

$$\begin{aligned}
\mathcal{R}^{(+)}(\boldsymbol{\rho}_{\mathbf{k}_S}) \approx & |V_{P_1}|^2 + |V_{P_2}|^2 \\
& + 2|V_{P_1}||V_{P_2}||\mathcal{T}(\boldsymbol{\rho}_{\tilde{\mathbf{k}}_I})| \cos(\arg[\mathcal{T}(\boldsymbol{\rho}_{\tilde{\mathbf{k}}_I})]), \quad (19a)
\end{aligned}$$

$$\begin{aligned}
\mathcal{R}^{(-)}(\boldsymbol{\rho}_{\mathbf{k}_S}) \approx & |V_{P_1}|^2 + |V_{P_2}|^2 \\
& - 2|V_{P_1}||V_{P_2}||\mathcal{T}(\boldsymbol{\rho}_{\tilde{\mathbf{k}}_I})| \cos(\arg[\mathcal{T}(\boldsymbol{\rho}_{\tilde{\mathbf{k}}_I})]). \quad (19b)
\end{aligned}$$

Equations (19) imply that an image of an absorptive object ($\arg[\mathcal{T}(\boldsymbol{\rho}_{\mathbf{k}_I})] = 0$) and as well as of a phase object ($|\mathcal{T}(\boldsymbol{\rho}_{\mathbf{k}_I})| = 1$) would appear in the camera for both constructive and destructive interferences (see [11], Fig. 3a). It further follows from Eqs. (19) that apart from a proportionality constant

$$\mathcal{R}^{(+)}(\boldsymbol{\rho}_{\mathbf{k}_S}) - \mathcal{R}^{(-)}(\boldsymbol{\rho}_{\mathbf{k}_S}) \approx |\mathcal{T}(\boldsymbol{\rho}_{\tilde{\mathbf{k}}_I})| \cos(\arg[\mathcal{T}(\boldsymbol{\rho}_{\tilde{\mathbf{k}}_I})]), \quad (20)$$

implying the background effect due to presence of the terms $|V_{P_1}|^2$ and $|V_{P_2}|^2$ can be eliminated by subtracting the photon counting rate obtained with destructive interference from that obtained with constructive interference (see [11], Fig. 3d). It also follows from Eqs. (19) that

$$\mathcal{R}^{(+)}(\boldsymbol{\rho}_{\mathbf{k}_S}) + \mathcal{R}^{(-)}(\boldsymbol{\rho}_{\mathbf{k}_S}) \approx 2(|V_{P_1}|^2 + |V_{P_2}|^2). \quad (21)$$

This means that summing up the photon counting rates obtained by constructive and destructive interferences removes the image (see [11], Fig. 3c). Clearly, even if one uses an absorptive object that completely blocks the beam I_1 , the summation of the photon counting rates does not change. The fact that the information of the object appears only in the interference term shows that the imaging process is purely quantum mechanical in nature; this point is discussed later in further details.

It is clear from the preceding discussion that a point $\boldsymbol{\rho}_{\tilde{\mathbf{k}}_I}$ in the object plane is imaged at the point $\boldsymbol{\rho}_{\mathbf{k}_S}$ in the image plane, where $\boldsymbol{\rho}_{\tilde{\mathbf{k}}_I}$ is the point at which a classical plane wave with wave vector $\tilde{\mathbf{k}}_I$ would be focused by the lens L1 [see Fig. 3(a)] and $\boldsymbol{\rho}_{\mathbf{k}_S}$ is the point where the plane wave characterized by \mathbf{k}_S would be focused by L0. Since $\tilde{\mathbf{k}}_I$ is the mirror image of the wave vector \mathbf{k}_I with respect to the optical axis [see Fig. 3(b)] and \mathbf{k}_I is related to \mathbf{k}_S by the phase matching condition $\mathbf{k}_I \approx \mathbf{k}_P - \mathbf{k}_S$, the image that appears on the camera is not inverted [23].

D. Image Magnification

So far we have neglected the effect of refraction at the crystal surface. However, one needs to consider this effect in order to obtain a correct value of the magnification. The wave vectors \mathbf{k}_S and $\tilde{\mathbf{k}}_I$ used thus far represent plane waves outside the crystals. The mirror image of $\tilde{\mathbf{k}}_I$ with respect to the optical axis z is \mathbf{k}_I [Fig. 3(b)]. Suppose that the plane waves with wave vectors \mathbf{k}_S and \mathbf{k}_I are represented inside the crystal by \mathbf{k}_S'' and \mathbf{k}_I'' , respectively. The phase matching condition can now be expressed as

$$\mathbf{k}_S'' + \mathbf{k}_I'' \approx \mathbf{k}_P'', \quad (22)$$

where \mathbf{k}_P'' is the wave vector of the pump field inside the crystal. If \mathbf{k}_S'' and \mathbf{k}_I'' make angles θ_S'' and θ_I'' , respectively, with \mathbf{k}_P'' which is along the optical axis, it follows from Eq. (22) that

$$\bar{\omega}_S n_S |\sin \theta_S''| \approx \bar{\omega}_I n_I |\sin \theta_I''|. \quad (23)$$

Let us choose two points on the object which are represented by two-dimensional position vectors $\boldsymbol{\rho}_{\tilde{\mathbf{k}}_I}$ and $\boldsymbol{\rho}_{\tilde{\mathbf{k}}_I}'$. Suppose that their images at the camera are represented by the two-dimensional position vectors $\boldsymbol{\rho}_{\mathbf{k}_S}$ and $\boldsymbol{\rho}_{\mathbf{k}_S}'$, respectively. The magnification is defined by the well known formula

$$M = \frac{|\boldsymbol{\rho}_{\mathbf{k}_S} - \boldsymbol{\rho}_{\mathbf{k}_S}'|}{|\boldsymbol{\rho}_{\tilde{\mathbf{k}}_I} - \boldsymbol{\rho}_{\tilde{\mathbf{k}}_I}'|}, \quad (24)$$

where its positive sign implies that the image is not inverted. As already mentioned, the origins in the object and the image planes are chosen at the points O and O' where the corresponding optical axes (beam axes) meet the respective planes [see Figs. 3(a) and 4]. It readily follows from the theory presented in Section III C that O' is the image of O . By choosing the points $\boldsymbol{\rho}_{\tilde{\mathbf{k}}_I}'$ and $\boldsymbol{\rho}_{\mathbf{k}_S}'$ at O and O' respectively, we reduce Eq. (24) to the simplified form

$$M = \frac{|\boldsymbol{\rho}_{\mathbf{k}_S}|}{|\boldsymbol{\rho}_{\tilde{\mathbf{k}}_I}|}. \quad (25)$$

If the signal plane wave \mathbf{k}_S , which is focused by the lens L1 at the point $\boldsymbol{\rho}_{\mathbf{k}_S}$, makes an angle θ_S with the optical axis z' (Fig. 4), one has in the small-angle approximation $|\boldsymbol{\rho}_{\mathbf{k}_S}| = |f_0 \tan \theta_S| \approx f_0 |\theta_S|$. Similarly, one can show that $|\boldsymbol{\rho}_{\tilde{\mathbf{k}}_I}| \approx f_I |\theta_I|$, where θ_I is the angle made by the wave vector $\tilde{\mathbf{k}}_I$ with the optical axis [Fig. 3(a)]. It now follows from Eq. (25) that

$$M = \frac{f_0 |\theta_S|}{f_I |\theta_I|}. \quad (26)$$

Since \mathbf{k}_S and \mathbf{k}_I are related to \mathbf{k}_S'' and \mathbf{k}_I'' , respectively, by refraction at the crystal surface, using Snell's law one obtains

$$n_S \sin \theta_S'' = n_0 \sin \theta_S, \quad n_I \sin \theta_I'' = n_0 \sin \theta_I, \quad (27)$$

where we have used the fact that \mathbf{k}_I and $\tilde{\mathbf{k}}_I$ make the same angle with the optical axis [Fig. 3(b)] and the refractive index of air (n_0) has practically the same value for signal and idler. From Eqs. (23) and (27), it immediately follows that $\bar{\omega}_S |\sin \theta_S| \approx \bar{\omega}_I |\sin \theta_I|$. In the small-angle limit, we thus obtain

$$\bar{\omega}_S |\theta_S| \approx \bar{\omega}_I |\theta_I|. \quad (28)$$

From Eqs. (26) and (28) one finds that

$$M = \frac{f_0 \bar{\omega}_I}{f_I \bar{\omega}_S} = \frac{f_0 \bar{\lambda}_S}{f_I \bar{\lambda}_I}. \quad (29)$$

Clearly, magnification of the imaging system depends on the ratio of the average wavelength of the signal to that of the idler. The dependence of the magnification on both wavelengths is a remarkable feature of our imaging process.

IV. CONCLUSION

We have theoretically analyzed a recently demonstrated [11] quantum imaging technique. Although the experimental setup resembles an ordinary two-arm interferometer, the principle behind the imaging is purely quantum mechanical. If one imagines a classical two-arm interferometer in one of whose arms an absorptive object is placed, both the interference term and the intensity contribution from the arm containing the object would depend on the transmissivity of the object. In our experiment, on the other hand, the intensity contribution from any of the crystals does not depend on the transmissivity of the object. It is evident from Eqs. (19) that the information of the object is present *only* in the interference term. This also shows that the interference of signal beams is not due to the effect of induced emission (see also [12, 24]). This interference can only be explained by indistinguishability of the signal photon paths and hence the imaging process is directly related to wave-particle duality of photons.

In this context, let us also have a close look at Eq. (13), which provides us with an expression for the quantum state $|\Psi\rangle$ that has been used for explaining the imaging process. Since the pump source used in the experiment is a narrow-band laser, this state is obtained (see Appendix 1) from the tensor product of the individual states, $|\psi_1\rangle$ and $|\psi_2\rangle$, generated by the crystals under the alignment-condition imposed by Eq. (11). This tensor product together with the alignment-condition implies the effect of induced emission. However, when the higher order terms present in $|\psi_1\rangle$ and $|\psi_2\rangle$ can be neglected, the state $|\Psi\rangle$ becomes identical with a state obtained by linear superposition of $|\psi_1\rangle$ and $|\psi_2\rangle$ under the same alignment-condition (see Appendix 1). Since such a superposition is only allowed when there is no effect of induced emission, it is clear that photons generated by spontaneous parametric down conversion play the key role in our imaging process [25].

Finally, although it is obvious, we would like to point out that the principle of our imaging also works if an entirely different lens system (or no lens system) is used in the experiment. A different lens system would only lead to a different value of the image magnification. Equation (29) shows that this magnification is equal to the product of two ratios: the ratio of focal lengths (f_0/f_I) and the ratio of wavelengths ($\bar{\lambda}_S/\bar{\lambda}_I$). The most remarkable feature of this result is the presence of two mean wavelengths in the formula of magnification. This is a consequence of (a) the fact that the object is illuminated by photons of one mean wavelength while the camera detects photons of the other wavelength and (b) the phase-matching condition [see Eq. (23)]. The use of a different lens system in the setup might lead to a different expression for the image magnification; however, a dependence on two average wavelengths would always be present.

Acknowledgements

The authors thanks M. Horne for many discussions. This project was supported by ÖAW, the European Research Council (ERC Advanced grant no. 227844 “QIT4QAD”, and SIQS grant no. 600645 EU-FP7-ICT), and the Austrian Science Fund (FWF) with SFB F40 (FOQUS) and W1210-2 (CoQus).

Appendix 1

In this appendix, we illustrate the procedure used for obtaining Eq. (13). We present a single-mode analysis, because the procedure does not change when all the modes present in the quantized fields are considered. The single-mode and scalar version of Eq. (7) can be represented in the form

$$|\psi_j\rangle = |\text{vac}\rangle + G_j |1\rangle_{S_j} |1\rangle_{I_j} + \dots, \quad (30)$$

where $j = 1, 2$, the time dependence is suppressed, the coefficients are collectively denoted by G_j and the dots represent higher order terms containing higher powers of G_j .

The single-mode version of Eq. (11) is given by

$$\hat{a}_{I_2} = [\mathcal{T}\hat{a}_{I_1} + \mathcal{R}'\hat{a}_0] e^{i\phi_I}. \quad (31)$$

From Eq. (31), one immediately obtains that

$$|1\rangle_{I_2} = [\mathcal{T}^* |1\rangle_{I_1} |0\rangle_0 + \mathcal{R}'^* |0\rangle_{I_1} |1\rangle_0] e^{-i\phi_I}. \quad (32)$$

Now using Eqs. (30) and (32), one can write

$$|\psi_1\rangle = |\text{vac}\rangle + G_1 |1\rangle_{S_1} |1\rangle_{I_1} |0\rangle_{S_2} |0\rangle_0 + \dots \quad (33a)$$

$$|\psi_2\rangle = |\text{vac}\rangle + G_2 e^{-i\phi_I} [\mathcal{T}^* |0\rangle_{S_1} |1\rangle_{I_1} |1\rangle_{S_2} |0\rangle_0 + \mathcal{R}'^* |0\rangle_{S_1} |0\rangle_{I_1} |1\rangle_{S_2} |1\rangle_0] + \dots \quad (33b)$$

Since both crystals are pumped by beams generated by a laser source (not a single photon source), the quantum state of light in the system is given by $|\Psi\rangle = |\psi_1\rangle |\psi_2\rangle$, i.e., by

$$\begin{aligned} |\Psi\rangle = & |\text{vac}\rangle + G_1 |1\rangle_{S_1} |1\rangle_{I_1} |0\rangle_{S_2} |0\rangle_{I_2} \\ & + G_2 e^{-i\phi_I} [\mathcal{T}^* |0\rangle_{S_1} |1\rangle_{I_1} |1\rangle_{S_2} |0\rangle_0 \\ & + \mathcal{R}'^* |0\rangle_{S_1} |0\rangle_{I_1} |1\rangle_{S_2} |1\rangle_0] \\ & + \text{higher order terms}, \end{aligned} \quad (34)$$

where the higher order terms contains higher second or higher powers of the coefficients G . Since the rate of down conversion is very small, the these higher order terms can be neglected. Hence the state $|\Psi\rangle$ can be approximated by (neglecting the normalization coefficients)

$$\begin{aligned} |\Psi\rangle \approx & |\text{vac}\rangle + G_1 |1\rangle_{S_1} |1\rangle_{I_1} |0\rangle_{S_2} |0\rangle_{I_2} \\ & + G_2 e^{-i\phi_I} [\mathcal{T}^* |0\rangle_{S_1} |1\rangle_{I_1} |1\rangle_{S_2} |0\rangle_0 \\ & + \mathcal{R}'^* |0\rangle_{S_1} |0\rangle_{I_1} |1\rangle_{S_2} |1\rangle_0]. \end{aligned} \quad (35)$$

Equation (13) is the multi-mode version of Eq. (35).

It is to be noted that the form of $|\Psi\rangle$ given by Eq. (35) can also be obtained by linear superposition of the states given by Eqs. (33a) and (33b), if one neglects the higher order terms. It is thus clear that if the experimental

conditions are such that the contribution of these higher order terms is much smaller than that of the first order terms to a measurement of our interest, the measurement would yield the same result as in a case when the state $|\Psi\rangle$ must be obtained by superposing $|\psi_1\rangle$ and $|\psi_2\rangle$.

References and Notes

- [1] N. Bohr, "Discussion with Einstein on epistemological problems in atomic physics," Albert Einstein: Philosopher Scientist, vol. 1, P. A. Schilpp Ed. (1949).
- [2] N. Bohr, "Das Quantenpostulat und die neuere Entwicklung der Atomistik," *Naturwissenschaften* **16**, 245-257 (1928).
- [3] J.-M. Le y-Leblond, "A Quantum Credo," *Physica B* **151**, 378-380 (1988).
- [4] The lowest-order interference has been referred to as both second-order [19] and first-order [21] in the literature.
- [5] R. P. Feynman, R. B. Leighton and M. Sands, *The Feynman Lectures on Physics, Vol. III*, (Addison-Wesley Publishing Company, New York, USA 1966).
- [6] D. M. Greenberger and A. Yasin, "Simultaneous wave and particle knowledge in a neutron interferometer," *Phys. Lett. A* **128**, 391-394 (1988).
- [7] L. Mandel, "Coherence and indistinguishability," *Opt. Lett.* **16**, 1882 (1991).
- [8] G. Jaeger, A. Shimony and L. Vaidman, "Two interferometric complementarities," *Phys. Rev. A* **51**, 54 (1995).
- [9] B.-G. Englert, "Fringe visibility and which-way information: an inequality," *Phys. Rev. Lett.* **77**, 2154 (1996).
- [10] M. Arndt, O. Nairz, J. Vos-Andreae, C. Keller, G. v.d. Zouw and A. Zeilinger, "Waveparticle duality of C_{60} molecules," *Nature* **401**, 680-682 (1999).
- [11] G. B. Lemos, V. Borish, G. D. Cole, S. Ramelow, R. Lapkiewicz and A. Zeilinger, "Quantum imaging with undetected photons," *Nature* **512**, 409-412 (2014).
- [12] X. Y. Zou, L. J. Wang and L. Mandel, "Induced Coherence and Indistinguishability in Optical Interference," *Phys. Rev. Lett.* **67**, 318-321 (1991).
- [13] L. J. Wang, X. Y. Zou and L. Mandel, "Induced Coherence without Induced Emission," *Phys. Rev. A* **44**, 4614-4622 (1991).
- [14] C. K. Hong and L. Mandel, "Theory of parametric down conversion of light," *Phys. Rev. A* **31**, 2409-2418 (1985).
- [15] Quantization of electromagnetic fields inside a nonlinear crystal is a non-trivial problem. However, when the nonlinearities are not high, the field is often represented in a form which is analogous to that of the free quantized field (see, for example, [19], Ch. 22).
- [16] R. Ghosh, C. K. Hong, Z. Y. Ou and L. Mandel, "Interference of two photons in parametric down conversion," *Phys. Rev. A* **34**, 3962-3968 (1985).
- [17] S. P. Walborn, C. H. Monken, S. P dua and P. H. Souto Ribeiro, "Spatial correlations in parametric down-conversion," *Phys. Rep.* **495**, 87-139 (2010).
- [18] We assume that almost the entire volume of each crystal is illuminated by the pump beam.
- [19] L. Mandel and E. Wolf, *Optical Coherence and Quantum Optics* (Cambridge, Cambridge University Press, 1995).
- [20] The photons are detected outside the crystals, whereas the phase matching conditions represent criteria inside the crystals. Hence the signal wave vectors used in Eq. (12) are related to the ones used in Eq. (13) by the refraction that occurs at the crystal surface. In this subsection, we neglect the effect of this refraction for simplicity. This effect is considered in Section III D, where we determine the image magnification.
- [21] R. J. Glauber, "The quantum theory of optical coherence" *Phys. Rev.* **130**, 2529 (1963).
- [22] When constructive interference is observed in one of the outputs of the beam splitter, destructive interference occurs in the other output. Because of this changing values of ϕ_P from ϕ_{PC} to ϕ_{PD} can be avoided during the experiment by collecting both outputs of the beam splitter. However, it must be noted that coincidence counts are never detected in this experiment. Detection of coincidence counts are required for investigating higher order interference phenomena (see, for example, [13, 26]).
- [23] It is to be noted that by changing the lens system in the experimental setup, it is possible to change the relation between $\tilde{\mathbf{k}}_I$ and \mathbf{k}_I but not the phase matching condition. In principle, it is thus possible to obtain an inverted image by using a different lens system.
- [24] H. M. Wiseman and K. M lmer, "Induced coherence with and without induced emission," *Phys. Lett. A* **270**, 245-248 (2000).
- [25] The higher order terms present in $|\psi_1\rangle$ and $|\psi_2\rangle$ contain higher (4 or more) photon states. Because of this the effect of induced emission can be observed in certain phenomena (see, for example, [27]) where the lower photon-number states do not contribute (i.e., one can no longer neglect the higher order terms).
- [26] A. V. Burlakov, D. N. Klyshko, S. P. Kulik and M. V. Chekhova, "Fourth-order interference between independent biphotons," *JETP Lett.* **69**, 831-838 (1999).
- [27] B. H. Liu, F. W. Sun, Y. X. Gong, Y. F. Huang, Z. Y. Ou and G. C. Guo, "Investigation of the role of indistinguishability in photon bunching and stimulated emission," *Phys. Rev. A* **79**, 053846 (2009).